ChemComm

COMMUNICATION

Cite this: *Chem. Commun.*, 2017, 53, 12294

Received 13th June 2017,
Accepted 23rd October 2017

DOI: 10.1039/c7cc04499b

rsc.li/chemcomm

Continuous-feed nanocasting process for the synthesis of bismuth nanowire composites†

K. Vandaele, [a] J. P. Heremans,[bcd] I. Van Driessche,[a] P. Van Der Voort [a] and K. De Buysser *[a]

We present a novel, continuous-feed nanocasting procedure for the synthesis of bismuth nanowire structures embedded in the pores of a mesoporous silica template. The immobilization of a bismuth salt inside the silica template from a diluted metal salt solution yields a sufficiently high loading to obtain electrically conducting bulk nanowire composite samples after reduction and sintering the nanocomposite powders. Electrical resistivity measurements of sintered bismuth nanowires embedded in the silica template reveal size-quantization effects.

Thermoelectrics could play an important role in waste heat recovery and solid-state cooling as they possess the ability to convert heat directly to electricity and *vice versa*.[1,2] The advantages of thermoelectrics include quiet operation, no mechanical moving parts, and a long lifetime. However, the limiting factor preventing the large-scale production of thermoelectrics for both power production and solid-state cooling is their low efficiency. A material's efficiency is described by the figure of merit, denoted zT, and is defined as: $zT = S^2T/\rho\kappa$, with S the Seebeck coefficient, ρ the electrical resistivity, and κ the thermal conductivity.

Pioneering work by Hicks and Dresselhaus[3] theoretically predicted that nanostructured thermoelectrics, could have an enhanced zT value compared to their bulk counterparts.[3,4] Such increase of zT was predicted in cylindrical Bi nanowires by Lin *et al.*[5] The synthesis of Bi nanowires by pressure injection[6] of a melt in porous, anodized alumina was reported Zhang *et al.*, while Heremans *et al.* reported the synthesis of Bi nanowires by the impregnation of Bi vapour in an alumina template.[7] Attempts at making Bi nanowire thermoelectrics[7] have resulted in large thermopowers, but comparatively small zTs. One issue has been that no $Bi_{1-x}Sb_x$ nanowires could be prepared by conventional methods due the large difference in melting point and vapour pressure between Bi and Sb, whereas theory[8] predicted superior performance in these alloy wires. In addition, the high thermal conductivity of an alumina matrix causes parasitic thermal losses, deteriorating the zT.

A suitable chemical route to synthesize non-siliceous nanostructured and mesoporous materials is by means of a hard template replication method, known as nanocasting.[9,10] Typically, the pores of mesoporous silica are used as a nano-mold or template. Since mesoporous silica materials possess pores with dimensions ranging from approximately 2 to 50 nm, they are perfect as a template material to synthesize Bi nanowire composites with diameters well below the threshold of 50 nm to observe a semimetal-to-semiconductor transition.[5]

A crucial step in the nanocasting replication process is the impregnation of the precursor material inside the template's pores and the conversion of that precursor to the target material. Typically, a metal salt dissolved in ethanol or water is loaded inside the mesoporous template through conventional solvent impregnation,[11] dry impregnation or incipient wetness,[12] double solvent,[13,14] or evaporation-induced impregnation method, and subsequently subjected to a thermal treatment.[9,10,15–17] The replicated mesoporous material is obtained after template removal through chemical etching with NaOH or HF. However, problems associated with the current impregnation methods of mesoporous templates include the low filling degree, inhomogeneous filling of the pores, or the deposition of precursor material on the external surface of the porous template. In many cases, multiple loading steps are required to obtain an acceptable degree of loading.[11,18,19] Ordered, mesoporous silica templates were used by Xu *et al.* for the synthesis of Bi nanowires by the decomposition of triphenylbismuth in supercritical toluene.[20] However, only small quantities of material were obtained.

In the present work, a scalable, continuous-feed impregnation process based on the two-solvent impregnation method[21] was used (Fig. 1). This process was developed to fill the pores of a mesoporous silica template with bismuth metal salt by impregnating the template with a diluted acidic precursor solution. A low-temperature reduction treatment (220 to 230 °C) allowed the conversion of the impregnated bismuth salt to metallic bismuth nanowires confined in the template's pores. Powder processing

[a] *Department of Inorganic and Physical Chemistry, Ghent University, Krijgslaan 281-S3, 9000 Gent, Belgium. E-mail: Klaartje.DeBuysser@ugent.be*
[b] *Department of Mechanical and Aerospace Engineering, Columbus, Ohio, 43210, USA*
[c] *Department of Physics, The Ohio State University, Columbus, Ohio, 43210, USA*
[d] *Department of Materials Science and Engineering, The Ohio State University, Columbus, Ohio, 43210, USA*

† Electronic supplementary information (ESI) available. See DOI: 10.1039/c7cc04499b

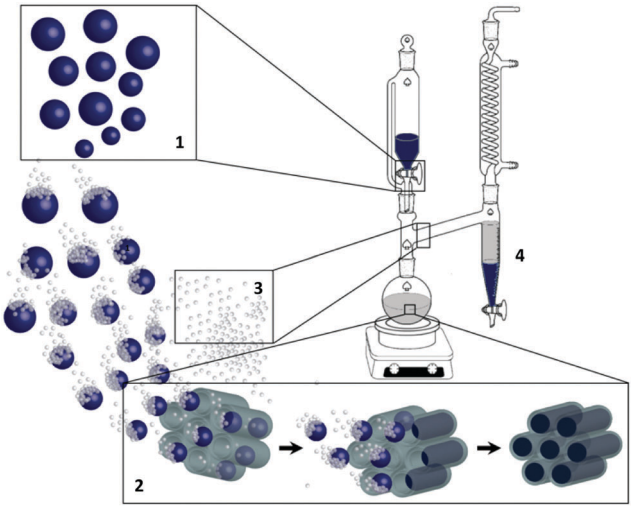

Fig. 1 Schematic of the continuous-feed impregnation procedure in refluxing *n*-octane (bp. 125 °C). (1) The aqueous precursor solution is added to the silica/*n*-octane dispersion using an addition funnel or syringe pump. (2) The polar precursor solution and *n*-octane from a two-phase system. Meanwhile, the precursor infiltrates the silica template through capillary impregnation. (3) As the impregnation is performed in refluxing *n*-octane, the water boils off and the diluted precursor solution inside the pores becomes more concentrated until all water is removed and only the precursor salt remains. Partial decomposition of the precursor salt may occur. (4) The aqueous solution is collected by means of a Dean–Stark separator.

techniques allowed the synthesis of bulk-sized samples composed of Bi nanowires, referred to as bulk nanowire composites. Electrical resistivity measurements were performed to identify size quantization effects in the bulk nanowire composite.

The two-solvent impregnation method[21] (Fig. S3, ESI†) consists of the addition of precursor solution in an amount equal to the pore volume of the template in a dispersion of the template in hexane. In the process described here, the precursor solution is added continuously to a dispersion of the mesoporous silica template in refluxing toluene or *n*-octane. By means of a Dean–Stark separator, the aqueous phase is eliminated from the system, leading to the immobilization of the metal precursor salt inside the template's pores. All chemicals are listed in the ESI† (Section 1).

In a typical synthesis, 1 g SBA-15 or KIT-6 mesoporous silica (Section 3, ESI†) with a pore volume of 1 $cm^3\ g^{-1}$ was dispersed in 100 mL *n*-octane in a 250 mL fluoropolymer (PFA) round bottom flask (Section 4, ESI†). The amount of metal salt required to fill the template's pores was derived based on the template's pore volume and the density of the precursor salt. For the impregnation of $BiCl_3$, the precursor solution was prepared by dissolving 3.5 g Bi_2O_3 in 12 mL 36 w% HCl and 24 mL H_2O. The precursor solution was added to the dispersion of silica in *n*-octane at a rate of 4 mL h^{-1} using a syringe pump, while the non-polar solvent was refluxing (Fig. S4, ESI†). All studied samples are listed in Table S1 (ESI†). The impregnated silica powder was collected through filtration and subsequently reduced in a sealable flow furnace at 230 °C for 12 h in a N_2–5% H_2 gas flow mixed with hydrazine vapour. The hydrazine vapour was carried through the furnace by bubbling the N_2–5% H_2 gas through a hydrazine monohydrate solution (Fig. S7, ESI†). The Bi–SiO_2 nanowire composite powder was removed from the flow furnace inside an argon glovebox, and approximately 2 g sample was transferred to a 10 mm ∅ graphite die, which was sealed with rubber glue to avoid oxidation when transferred to the spark plasma sintering (SPS) device. The nanowire composite powder was sintered at 230 °C for 20 min in a vacuum under a uniaxial pressure of 50 MPa. The sample preparations for four-probe electrical transport measurements and mounting inside the cryostat were performed in an argon glovebox. Typical sample dimensions for electrical transport measurements were 1.5 × 1 × 7 mm. For N_2 sorption analysis, the silica template of the reduced Bi–SiO_2 powder was dissolved in a 1 mol L^{-1} NaOH solution for 3 h. The mesoporous Bi powder was isolated by centrifugation and washed four times with water.

The X-ray powder diffraction (XRPD) patterns in Fig. S10 (ESI†) show that the bismuth precursor salt reduced to bismuth at 230 °C for 12 h in the presence of hydrazine vapour. When measured under argon atmosphere, no secondary phases were observed. However, upon removing the tape, which sealed the sample from air, the XRPD pattern indicates the presence of $Bi_2O_{2.5}$, which formed within seconds. KIT-6 mesoporous silica, with a 3D interconnected mesopore system, was used as template for the preparation of mesoporous bismuth powder for N_2 physisorption measurements and for electric transport measurements. Mesoporous bismuth, was obtained after chemical etching of the KIT-6 silica template. A BET surface area of 20 $m^2\ g^{-1}$ and 13 $m^2\ g^{-1}$ was obtained when $Bi(NO_3)_3$ and $BiCl_3$, respectively, were used as precursor salts (Fig. S11, ESI†). The pore volumes were 0.14 and 0.06 $cm^3\ g^{-1}$, respectively.

SBA-15 mesoporous silica, which possesses hexagonally packed, cylindrical mesopores, was used as template for the TEM analysis shown in Fig. 2. The TEM images depict oxidized bismuth nanowires (due to sample preparation for TEM) with a diameter between 5 and 10 nm confined in the template's pores (a and c) and the replicated nanowires after etching the template (b and d). The appearance of the nanowires depends on the precursor salt used. Namely, for $Bi(NO_3)_3$, rough nanowires were obtained, whereas smooth wires were obtained for $BiCl_3$. The latter also forms a melt at approximately 228 °C according to DTA shown in Fig. S6 (ESI†). The theoretical volume fractions of Bi confined in the pores are 12 v% and 30 v% for $Bi(NO_3)_3$ and $BiCl_3$, respectively.

Fig. 3 depicts the carrier concentration of a sintered Bi–SiO_2 (KIT-6) nanowire composite sample as function of $1/2kT$. By fitting the carrier concentration for an intrinsic semiconductor through the data points, a band gap of 45 meV was calculated. Fig. 4 compares the electrical resistivity of bulk Bi with that of Bi nanowire composites normalized by their value at 300 K. The data shows the occurrence of size-quantization effects in the nanowire composite samples, since the electrical resistivity behaviour follows a semiconducting behaviour instead of a metallic one, as in bulk Bi.

The loading of the pores changes significantly depending on the precursor salt used, given the difference in density and molecular weight of $Bi(NO_3)_3$ and $BiCl_3$. If we consider complete filling of the pores with the precursor salts, 12 v% and 30 v%, Bi can be deposited in the pores after reduction of $Bi(NO_3)_3$ and $BiCl_3$, respectively. How the loading could be further enhanced is shown in Table S2 (ESI†). KIT-6, a mesoporous silica template with an interconnected pore system, was used for the synthesis of mesoporous Bi. No high-BET surface area was obtained for either sample,

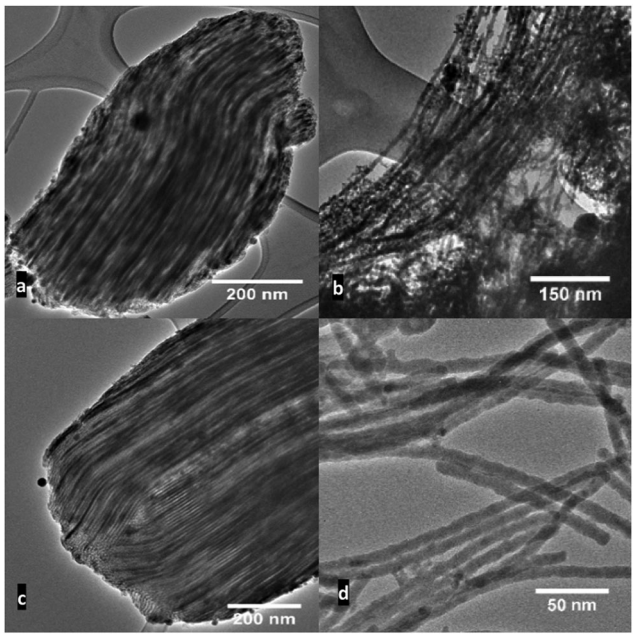

Fig. 2 (a) TEM image of SBA-15 filled with 12 v% Bi, prepared by the impregnation of $Bi(NO_3)_3{\cdot}5H_2O$ dissolved in 5 mol L^{-1} HNO_3, with toluene as non-polar solvent and reduced at 220 °C in a hydrazine loaded Ar–5% H_2 gas flow for 12 h. (b) Bi nanowires after chemical etching of the silica template of the sample in 1 mol L^{-1} NaOH solution for 3 h. (c) TEM image of SBA-15 filled with 30 v% Bi, prepared by the impregnation of $BiCl_3$ dissolved in a 4 mol L^{-1} HCl–80 v% MeOH solution, with *n*-octane as non-polar solvent and reduced at 220 °C in a hydrazine loaded Ar–5% H_2 gas flow for 12 h. (d) Bi nanowires after chemical etching of sample c. Note that Bi nanowires oxidize spontaneous in air, therefore the analysed samples referred to as Bi are oxidized.

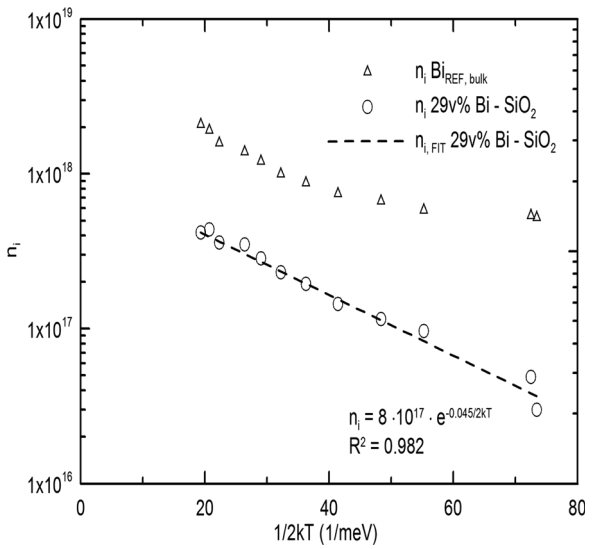

Fig. 3 Carrier concentration of bulk bismuth and 29 v% Bi–SiO_2 (KIT-6) nanowire composite sample as function of 1/2*kT*. The lower carrier concentration of the nanocomposite sample compared to bulk Bi can be attributed to size-quantization effects in the nanowires. The carrier concentration for the intrinsic semiconductor was derived by $n_i = n_0 e^{-Eg/2kT}$. The band gap obtained by the fit through the data points yields: E_g = 45 meV, which corresponds to Bi nanowires with diameter 20 nm according to Lin *et al.*[5] Note that all sample preparations and measurements were performed under inert atmosphere.

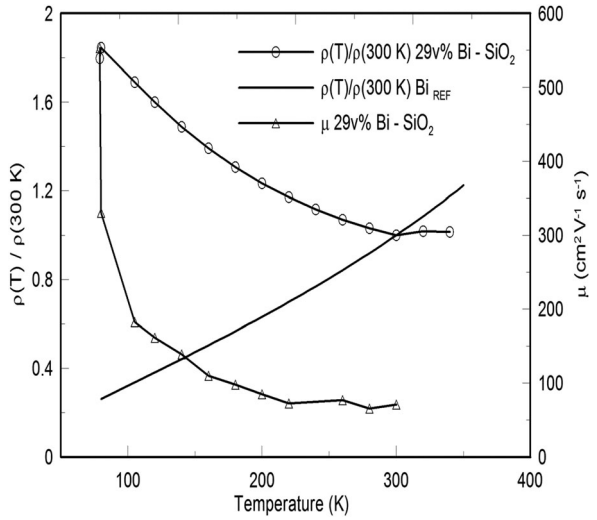

Fig. 4 Electrical resistivity of 29 v% Bi–SiO_2 nanowire composite sample and bulk bismuth normalized by their value at 300 K. Where the normalized resistivity of bulk Bi drops, and thus exhibits a metallic character when cooled down to 77 K, the relative resistivity of 29 v% Bi–SiO_2 increases, providing evidence for size-quantization effects in sintered bismuth nanowire composites. The carrier mobility is depicted on the right axis. Note that all sample preparations and measurements were performed under inert atmosphere.

which primarily is due to the high density of Bi (9.78 g cm^{-3}) and its low melting point (271.5 °C). Bismuth also can leach out of a template's pores during reduction of the bismuth salt. This was mostly observed for $BiCl_3$, as it also forms a melt at approximately 228 °C (Fig. S6, ESI†). We believe that the smooth nanowires in Fig. 2 were obtained specifically because of the formation that melt. The use of $BiCl_3$ as precursor was preferred since it can lead to a higher loading of Bi inside the template. This is particularly important for the synthesis of nanocomposites, as a sufficiently high loading of Bi in the template is required to form an electrical percolation path when the Bi–SiO_2 nanowire composite powder were sintered. For the same reason, the use of a silica template with 3D interconnected pore system (KIT-6) is preferred over a template with linear pores (SBA-15). Electric transport measurements were performed on a bulk nanowire composite sample using KIT-6 with a pore diameter of approximately 7 nm as silica template. Based on the amount of $BiCl_3$ precursor salt impregnated in the template, the estimated composition of the composite sample was 33 v% silica, 29 v% Bi nanowires and 38 v% voids.

Evidence of size quantization in the bismuth nanowire composites was obtained from measurements of the Hall effect (Fig. 3) and resistivity (Fig. 4) of the sintered samples. For the nanocomposites, the Hall resistivity is corrected for the volume fractions of Bi by using the effective medium theory[22] for the Hall effect; for approx. 30% Bi filling by volume, that correction is a factor of 2.2, does not affect the T-dependence nor the band gap. The inverse of the low-field (<1 Tesla) Hall slope R_H was interpreted to give the charge-carrier concentration *via* $n = (eR_H)^{-1}$ with *e* the electron charge. R_H was positive, so the dominant carriers are holes. Fig. 3 shows the temperature dependence of *n* measured on the sample (29 v% Bi–SiO_2), in an Arrhenius plot. A very clean, activated behavior is observed, following a law $n(T) = n_0 e^{-E_g/2k_BT}$ valid for intrinsic semiconductors, where E_g is the band gap of the

semiconductor. A mixture of very narrow nanowires with bulk-like Bi (which displays a metal-like conductivity) will not generate such a simple temperature-dependence. Furthermore, the charge-carrier concentration measured on the nanowire sample is an order of magnitude smaller than that (also shown in Fig. 3) of bulk Bi.[23] Finally, the value of E_g = 45 meV obtained from the Arrhenius plot in Fig. 3 corresponds very well to the theoretical value of the band gap opened by size-quantization effects in Bi nanowires of about 20 nm diameter, providing evidence of size quantization effects in the nanowire composites.

At first sight, the 20 nm diameter measured by electrical measurements appears to contradict the observation that the template's pores were 7 nm, which should correspond to a bandgap exceeding 100 meV. However, it has been observed experimentally[7] that conduction in nanowires of diameter smaller than 9 nm becomes localized. In contrast, no localization is observed in the sample measured here, as is illustrated by the resistivity data in Fig. 4. These data show a temperature dependence consistent with the decrease in carrier concentration, very different from bulk Bi (also shown) and conducive to mobilities (shown using the right-hand ordinate axes) of the order of 500 to 50 $cm^2\ V^{-1}\ s^{-1}$. Because there is always a statistical distribution of nanowire diameter, these observations lead to the conclusion that the conduction is dominated by nanowires with diameters near 20 nm with conduction in all the narrower wires simply localized. Indeed, there is a lower limit to the range of validity of the theoretical calculations by Lin *et al.*[5] set by the condition for Anerson localization:[24] the product $k_F \cdot l > 1$, where k_F is the Fermi wavevector and l is the electronic mean-free path, here limited by the wire diameter. For bulk Bi, k_F is given in ref. 25 to be very anisotropic with the smallest value $1 \times 10^8\ m^{-1}$, meaning that nanowires with diameters below 10 nm should not conduct. Because of quantization, the carrier concentration in the present sample is smaller still, leading to a smaller k_F; therefore, the minimum wire diameter must be larger, *e.g.* on the order of the observed 20 nm.

In conclusion, a facile nanocasting technique was developed for the synthesis of bismuth nanowire composites. By means of the continuous-feed nanocasting process and a low-temperature reduction treatment of the impregnated bismuth salt, we were able to synthesize bismuth nanowires embedded in the pores of a mesoporous silica powder. The nanocasting method enabled a sufficiently high loading of bismuth inside the pores of a 3D interconnected silica template to form electrically conducting nanowire composite samples. This provides the opportunity to fabricate a bulk material composed of nanowires with potentially enhanced thermoelectric properties. Evidence of size-quantization effects was obtained from electrical resistivity and carrier concentration data, which show the clear signature of semiconducting band conduction with an energy gap of 45 meV and no signs of localization. The results suggest several directions for further research, *e.g.* aliovalent doping and alloying Bi with Sb, as well as measurements of the thermoelectric properties of the material, in order to enhance the material's zT.

The authors would like to acknowledge funding of this research by the Flemish Government (Innovation Science and Technology project) and the Flanders Research Foundation (FWO). KV would like to thank Bin He and Prof. J. P. Heremans for many fruitful discussions, and in particular, thanks to Katrien Haustraete and Katrien De Keukeleere for all TEM measurements. KV also thanks María Dolores González Gómez for her support throughout the research and for making the abstract figure.

Conflicts of interest

There are no conflicts to declare.

Notes and references

1 L. E. Bell, Cooling, heating, generating power, and recovering waste heat with thermoelectric systems, *Science*, 2008, **321**(5895), 1457–1461.
2 F. J. DiSalvo, Thermoelectric cooling and power generation, *Science*, 1999, **285**(5428), 703–706.
3 L. D. Hicks and M. S. Dresselhaus, Thermoelectric figure of merit of a one-dimensional conductor, *Phys. Rev. B: Condens. Matter Mater. Phys.*, 1993, **47**(24), 16631–16634.
4 L. D. Hicks and M. S. Dresselhaus, Effect of quantum-well structures on the thermoelectric figure of merit, *Phys. Rev. B: Condens. Matter Mater. Phys.*, 1993, **47**(19), 12727–12731.
5 Y. M. Lin, X. Z. Sun and M. S. Dresselhaus, Theoretical investigation of thermoelectric transport properties of cylindrical Bi nanowires, *Phys. Rev. B: Condens. Matter Mater. Phys.*, 2000, **62**(7), 4610–4623.
6 Z. B. Zhang, *et al.*, Processing and characterization of single-crystalline ultrafine bismuth nanowires, *Chem. Mater.*, 1999, **11**(7), 1659–1665.
7 J. P. Heremans, *et al.*, Thermoelectric power of bismuth nanocomposites, *Phys. Rev. Lett.*, 2002, **88**(21), 216801.
8 S. Tang and M. S. Dresselhaus, Constructing Anisotropic Single-Dirac-Cones in $Bi_{1-x}Sb_x$ Thin Films, *Nano Lett.*, 2012, **12**(4), 2021–2026.
9 A. H. Lu and F. Schuth, Nanocasting: A versatile strategy for creating nanostructured porous materials, *Adv. Mater.*, 2006, **18**(14), 1793–1805.
10 A. Kong, *et al.*, Novel nanocasting method for synthesis of ordered mesoporous metal oxides, *J. Porous Mater.*, 2011, **18**(1), 107–112.
11 H. F. Yang and D. Y. Zhao, Synthesis of replica mesostructures by the nanocasting strategy, *J. Mater. Chem.*, 2005, **15**(12), 1217–1231.
12 Z.-J. Wang, Y. Xie and C.-J. Liu, Synthesis and Characterization of Noble Metal (Pd, Pt, Au, Ag) Nanostructured Materials Confined in the Channels of Mesoporous SBA-15, *J. Phys. Chem. C*, 2008, **112**(50), 19818–19824.
13 X. Huang, *et al.*, Effect of metal species on the morphology of metal (oxides) within mesochannels of SBA-15 *via* a double-solvent method, *Microporous Mesoporous Mater.*, 2015, **207**, 105–110.
14 X. Huang, *et al.*, Synthesis of confined Ag nanowires within mesoporous silica *via* double solvent technique and their catalytic properties, *J. Colloid Interface Sci.*, 2011, **359**(1), 40–46.
15 A. H. Lu, *et al.*, Taking nanocasting one step further: Replicating CMK-3 as a silica material, *Angew. Chem., Int. Ed.*, 2002, **114**(18), 3639–3642.
16 H. F. Yang, *et al.*, One-step nanocasting synthesis of highly ordered single crystalline indium oxide nanowire arrays from mesostructured frameworks, *J. Am. Chem. Soc.*, 2003, **125**(16), 4724–4725.
17 J. Roggenbuck, *et al.*, Mesoporous CeO_2: Synthesis by nanocasting, characterisation and catalytic properties, *Microporous Mesoporous Mater.*, 2007, **101**(3), 335–341.
18 E. Delahaye, *et al.*, "Nanocasting": Using SBA-15 silicas as hard templates to obtain ultrasmall monodispersed gamma-Fe_2O_3 nanoparticles, *J. Phys. Chem. B*, 2006, **110**(51), 26001–26011.
19 N. El-Hassan, *et al.*, SBA-15 silicas as hard templates for the nanocasting of oxide nanoparticles, *Annales De Chimie-Science Des Materiaux*, 2005, **30**(3), 315–326.
20 J. Xu, *et al.*, The formation of ordered bismuth nanowire arrays within mesoporous silica templates, *Mater. Chem. Phys.*, 2007, **104**(1), 50–55.
21 H. Yen, *et al.*, One-step-impregnation hard templating synthesis of high-surface-area nanostructured mixed metal oxides ($NiFe_2O_4$, $CuFe_2O_4$ and Cu/CeO_2), *Chem. Commun.*, 2011, **47**(37), 10473–10475.
22 D. J. Bergman and D. G. Stroud, *Phys. Rev. B: Condens. Matter Mater. Phys.*, 2000, **62**, 6603.
23 J. P. Issi, *Aust. J. Phys.*, 1979, **32**(6), 585–628.
24 A. A. Abrikosov, *Fundamentals of the theory of metals*, Elsevier Science Pub. Co., North-Holland, Amsterdam; New York, NY, USA, sole distributors for the USA and Canada, 1988.
25 V. S. Edelman, Properties of electrons in bismuth, *Soviet Physics Uspekhi*, 1977, **20**(10), 819–835.